Materials and Design 191 (2020) 108589

Contents lists available at ScienceDirect

Materials and Design

journal homepage: www.elsevier.com/locate/matdes

# Improving lignocellulose thermal stability by chemical modification with boric acid for incorporating into polyamide

Jingfa Zhang [a,b], Ahmed Koubaa [b], Dan Xing [b], Wanyu Liu [a], Qingwen Wang [c], XiangMing Wang [d], Haigang Wang [a,*]

[a] Key Laboratory of Bio-based Materials Science and Technology (Ministry of Education), Northeast Forestry University, Harbin 150040, PR China
[b] Université du Québec en Abitibi-Témiscamingue, Rouyn-Noranda, Québec J9X 5E4, Canada
[c] College of Materials and Energy, South China Agricultural University, Guangzhou 510642, PR China
[d] New Construction Materials, FPInnovations, Québec, Québec G1V 4C7, Canada

## HIGHLIGHTS

- Bio-composites based on engineering plastic were prepared by improving the thermal stability of lignocellulose.
- The thermal stability of lignocellulosic fiber was improved by boric acid modification.
- The chemical structure of lignocellulose changed because of the complexation reaction between boric acid and lignocellulose.
- Boric acid has a positive effect on the physical properties of the composites.

## GRAPHICAL ABSTRACT

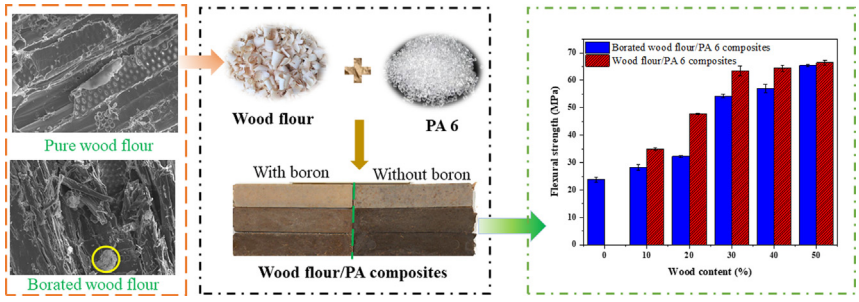


## ARTICLE INFO

*Article history:*
Received 26 November 2019
Received in revised form 17 February 2020
Accepted 19 February 2020
Available online 24 February 2020

*Keywords:*
Lignocellulose
Boric acid modification
Thermal stability
Polyamide 6
Polymer-matrix composites

## ABSTRACT

The preparation of bio-composites based on engineering plastic is always restricted by the low thermal stability of lignocellulose. In this study, the thermal stability of lignocellulose was improved by boric acid modification. Then, the borated lignocellulose was characterized to analyze the mechanism of involved in the improvement of thermal stability. Furthermore, the untreated and borated lignocellulose was combined with polyamide 6 to produce bio-composites. The effects of lignocellulose content and boric acid modification on the color, thermal stability and mechanical properties of the resulting composites were compared and analyzed. Boric acid protected lignocellulose from thermal degradation, increasing the lightness of the resulting composites. However, boric acid appeared to have a negative effect on the mechanical strength of the resulting composites. In summary, this study demonstrated that bio-composites based on engineering plastic could be prepared by improving the thermal stability of lignocellulose using a boric acid treatment.


## 1. Introduction

Bio-composites consisting of lignocellulosic fiber and thermoplastic have been among of the most attractive composites. It has been widely

* Corresponding author.
*E-mail address:* hgwang@nefu.edu.cn (H. Wang).

https://doi.org/10.1016/j.matdes.2020.108589

used in transportation, automotive, outdoor construction and decoration and other fields due to their advantages of low water absorption and recyclability [1,2]. They received considerable interest from both academia and industry because of their good environmental and economic benefits. However, there are several drawbacks to overcome for expanding future uses, such as low strength, poor creep behavior and thermal stability.

Compared to polyethylene or polypropylene, Polyamide 6 (PA 6), as an engineering plastic, has excellent mechanical properties, thermal properties, and chemical stability [1]. Furthermore, a great compatibility between PA 6 and lignocellulosic fillers can be obtained because of their similar hydrophilic nature [3]. Studies of lignocellulosic filler reinforced PA 6 have been increasingly reported in recent literature [4,5]. However, adding cellulose decreases the strength and elongation of composites and causes them to darken, because of the thermal degradation of the cellulose [6]. Although other papers have shown lignocellulosic fillers can increase the strength of composites, the challenge of the contradiction of the weak thermal stability of natural fibers and the high melting point of PA 6 is still present [7,8].

Hence, two methods were proposed to solve this problem: increasing the thermal stability of the lignocellulosic fibers and lowering the melting point of the polyamide 6. Plasma treatment, heat treatment, and hydroxide (NaOH) solution treatments are generally used to improve the thermal stability of lignocellulose [9,10]. On the other hand, lithium chloride is commonly used to lower the melting point of polyamides [11]. Lignocellulosic fiber/PA 6 composites modified by lithium chloride (LiCl) have been prepared. LiCl has a positive influence on the mechanical properties of the resulting bio-composite [3,5].

Boric acid has been widely used as preservative and flame retardant for wood and bio-composites [12,13]. The flame retardant mechanism of boric acid is usually believed to occur as a result of the cover effect of boron trioxide glass films. However, Wang et al. [14] thought than the hydrogen ion resulting from boric acid, can catalyze the pyrolysis of lignocellulose during burning and promote the forming of residual char. Moreover, a complexation of boric acid and nanocellulose occurs in an alkaline environment, resulting in good fire retardancy for nanocellulose aerogels [15]. Interestingly, boric acid treatments can also increase the thermal stability of lignocellulose, especially the onset temperature of the thermal degradation [16]. The thermal decomposition mechanism of pure lignocellulose has been studied widely [17,18]. However, there is a lack of understanding of the mechanism for the thermal degradation of the borated lignocellulose.

The main purpose of this study was to improve the thermal stability of wood flour by boric acid modification for use in into PA 6 resin biocomposites.

## 2. Materials and methods

### 2.1. Materials

Poplar-wood flour (30–80 mesh) was ground from poplar-veneer (Quebec, Canada). Heat stabilized super-tough polyamide 6 (PA 6) particles (Zytel® ST811HS NC010) with a density of 1.04 $g \cdot cm^{-3}$ were purchased from Polyone Co. Its melting point is 218 °C according to ISO 11357-1 (10 °C·$min^{-1}$). Analytical reagent grade boric acid powder was obtained from Sigma-Aldrich.

### 2.2. Wood flour modification

Wood flour was immersed in a boric acid solution of 5 wt% for 2 h. The ratio of solid to liquid was 1:4. Then, the treated wood flour was filtered and oven-dried at 103 °C for 24 h to reach a final moisture content below than 2 wt%. The control group was treated with deionized water and then oven-dried at 103 °C for 24 h to reach a moisture content below 2 wt%.

### 2.3. Preparation of wood flour/PA 6 composites

PA 6 particles were oven-dried at 90 °C for 10 h using before compounding. The wood flour/PA 6 composites were subsequently prepared in two steps: extrusion and pelleting followed by injection based on the composite formulations in Table S1. PA 6 particles and wood flour were compounded using a counter-rotating intermeshing conical twin-screw extruder (HAAKE PolyLab OS Rheodrive 7 with Rheomex OS extruding module, HAKKE, Germany). The screw speed was set to 50 rpm while barrel and die temperature was 210 °C.

Tensile and flexural specimens were injected by using an injection molding machine (MARS II 130/600, Haitian, China). The mold temperature was set at 80 °C, and the barrel temperature was 230 °C. Samples were molded with an injection pressure of 120 MPa and a 70 MPa holding pressure. The injection and holding time were 2 s and 10 s, respectively. All specimens were 3.20 mm thick.

### 2.4. Characterization

#### 2.4.1. Borated wood flour structure

Wood flour was analyzed with an attenuated total reflection Fourier transform infrared spectrophotometer (IRT racer-100, Shimadzu, Japan). Samples were scanned in the wave number range of 500–4000 $cm^{-1}$ with a resolution of 4 $cm^{-1}$. XRD spectra of wood flour before and after boric acid modification were measured using an X-ray diffractometer (D/max 2200; Rigaku, Japan) equipped with Ni-filtered Cu Kα radiation ($\lambda = 1.5406$ Å) at 40 kV and 30 mA. 2θ value ranged from 5° to 40° with a speed of 1°·$min^{-1}$. Furthermore, the crystallinity index (*CrI*) of samples was calculated according to the Segal method [19].

#### 2.4.2. Thermal stability

The thermal degradation behavior of wood flour and the wood flour/PA 6 composites was investigated by thermogravimetric analysis (TGA) using a TGA instrument (SDT Q600, TA, USA). The test temperature ranged from 50 °C to 600 °C at a heating rate of 10 °C·$min^{-1}$ under a nitrogen atmosphere.

Differential scanning calorimetry was used to investigate the melting temperatures and enthalpies of the resulting wood flour/PA 6 composites using a DSC instrument (Q50, TA, USA) under a nitrogen atmosphere with a sample weight of about 10 mg. Samples were heated to 240 °C and held for 3 min to remove their thermal history, and then cooled down to −30 °C with a cooling rate of 10 °C·$min^{-1}$. Finally, the temperature was increased to 240 °C again at a heating rate of 10 °C·$min^{-1}$.

#### 2.4.3. Color analysis

Specimens for color analysis were prepared using hot press. The surface color of the resulting composites was characterized using a CR-410 chroma meter (Konica Minolta, Japan) with a CIE Lab system. The color values, $L^*$, $a^*$, and $b^*$ were recorded at 5 random position per sample and averaged. The $\Delta L^*$, $\Delta a^*$, and $\Delta b^*$ were calculated based on the pure PA6 sample value (e.g. $\Delta L^* = L^*_1 - L^*_{control}$). The Euclidean distance ($\Delta E^*$), expressing the total color change, was calculated according to Eq. (1):

$$\Delta E^* = \sqrt{\left(\Delta L^{*2} + \Delta a^{*2} + \Delta b^{*2}\right)} \quad (1)$$

#### 2.4.4. Mechanical properties

Three-point bending tests were conducted according to the ASTM D-790 standard with a span-to-depth ratio of 16:1 and at a speed of 2 mm·$min^{-1}$. Test specimens (127 × 12.7 × 3.2 mm) were subjected to the bending test. Tensile properties were measured according to the ASTM D-638 standard using specimen Type I at a speed of 5 mm·$min^{-1}$. Each formulation was tested in 5 replicates.

*2.4.5. Morphological analysis*

The tested composites were frozen in liquid nitrogen for 10 min and then broken. Afterward, the fracture surfaces of the composites and wood flour were sputter coated with gold powder for scanning electron microscope observations (SEM SU1510, HITACHI, Japan) at an accelerating voltage of 10 kV. Meanwhile, the surface elements of the wood flour were analyzed using an energy dispersive spectrometer (X-MAX 20 $mm^2$, Oxford Instrument, UK).

## 3. Results and discussion

### *3.1. Properties of borated wood flour*

Borated wood flour was prepared after the complexation or esterification of poplar by boric acid under air atmosphere conditions (Scheme 1). Typical Fourier transform infrared spectroscopy (FTIR) spectrum of wood was observed while a large number of FTIR characteristic bands of tricoordinated and tetrahedra boron were visible in the borated wood flour spectra, as shown in Fig. 1a [20,21]. The esterification or complexation of the wood flour and boric acid were successfully proven by the new bands at 3200, 1380, 1340, 1280, 940 and 810 $cm^{-1}$, which can be attributed, respectively, to the stretching vibrations of the boric acid hydroxyl groups, B-O-B stretching vibrations, B-O-C stretching vibrations, stretching vibrations of the B—O bonds of 'boroxol rings', B-OH in-plane bending vibration, and stretching and bending vibrations of B—O in $BO_4^-$ tetrahedra [22]. In addition, the characteristic bands of benzene ring at 1600, 1500 and 1450 $cm^{-1}$ were covered by the valence vibrations bands of B-O-B and B-O-C. The 'boroxol rings' indicate the presence of self-polymerization of the boric acid in the borated wood flour. The complexation of the boric acid and nanocellulose were also observed in an alkali environment [15].

Furthermore, previous studies reveal that boric acid can react with polyhydroxy compounds, forming boric acid-polysaccharide complexes [23]. Lignin consisting of three alcohol monomers contains a lot of hydroxyls [18]. Thus, boric acid could complex with the alcohol hydroxyl of lignin or react with phenol hydroxyl in the way of esterification, as shown in Scheme 1. Therefore, one can see that wood can react with boric acid by complexation and esterification, which may increase the cross-linking degree of wood flour chemical structure.

The crystallinity (*CrI*) of wood flour decreased after boric acid treatments (Fig. S1). This decrease can be attributed to the swelling of the wood flour caused by the boric acid solution. First, boric acid attacked amorphous regions of the wood flour in a manner similar to water, then separate microfibrils, damaging the crystalline cellulose. On the other hand, the intermolecular and intramolecular hydrogen bonds of cellulose in the crystalline regions are disintegrated and replaced by B-O-C bonds during the treating process. Furthermore, the boric acid treatment also altered the crystal form of cellulose of wood flour (Fig. 1b). It is worth noting that a diffraction shoulder peak at $2\theta = 20.60°$, attributed to the $10\bar{1}$ diffraction crystal face of cellulose II [24], appeared in the borated wood flour XRD spectrum. This result indicates that boric acid partly changed the crystal form of cellulose, from cellulose I to cellulose II. Compared to cellulose I, Cellulose II is easier to form biochar during heating [25], which is conducive to fire retardancy and thermal stability of lignocellulosic materials. However, the strength of cellulose II is lower than that of cellulose I because of the small molecular weight of cellulose II [24]. Moreover, a diffraction peak associated to boric acid appeared in the XRD spectrum of the borated wood flour, indicating that some unreacted boric acid remains in the treated wood flour after treatment.

Wood flour thermal decomposition could be divided into two steps according to its derivative thermogravimetry (DTG) curve: depolymerization of hemicellulose and cellulose decomposition (Fig. 1c). However, three peaks were observed in the DTG curve of borated wood flour. The first decomposition peak occurring at about 150 °C is attributed to the dehydration resulted from the boric acid self-polymerization and the complexation of boric acid and hydroxyls [23]. The second step, in the range of 300–380 °C, is mainly due to the depolymerization of hemicellulose and cellulose. The degradation peaks of hemicellulose and cellulose were combined into one because of the improvement of hemicellulose thermal stability resulting from the increase in cross-linking of wood flour chemical structure. The final weight loss stage occurred at 380 °C to 450 °C, which was attributed to the degradation of the boric acid and wood flour complexes. Compared to wood flour, the thermal degradation rate of borated wood flour decreased whereas its char residue rate increased. These results show boric acid has a significant effect on the fire retardancy of lignocellulose, which is consistent with previous studies [12,26]. However, boric acid reduced the temperature at the maximum degradation rate. This decrease is related to the alteration of wood flour crystalline behavior. On the other hand, the free hydrogen ion, produced from the complexation of the boric acid and wood flour, catalyzes cellulose degradation [14].

The surface of the untreated wood flour was clean, and the pits were clear (Fig. S2). Some glassy materials were observed on the surface of the borated wood flour and some macro-fibrils were coated by a layer of boron compounds (Fig. 1d). This indicates that there was still some unreacted boric acid remaining on the borated wood flour, which is in agreement with the XRD results. The energy dispersive spectroscopy (EDS) revealed that the boron elements were

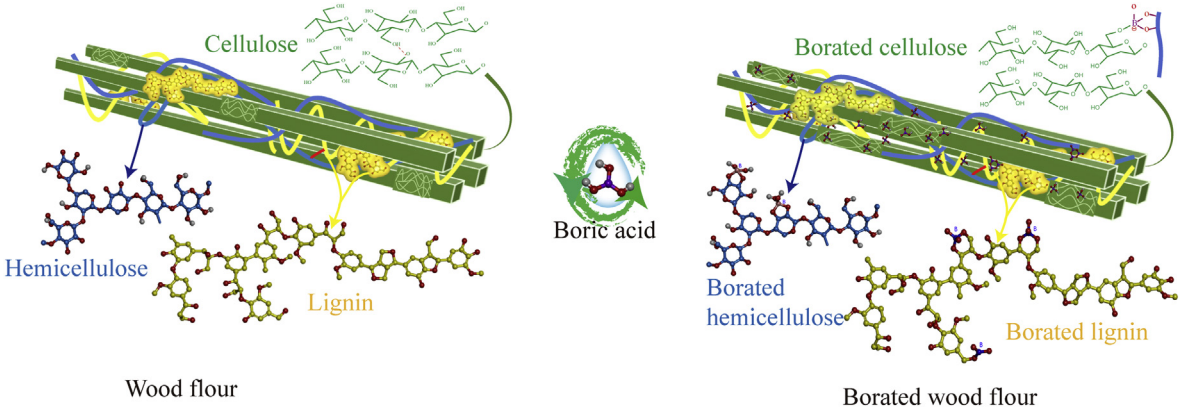


**Scheme 1.** Schematic illustration for the fabrication of borated wood flour.

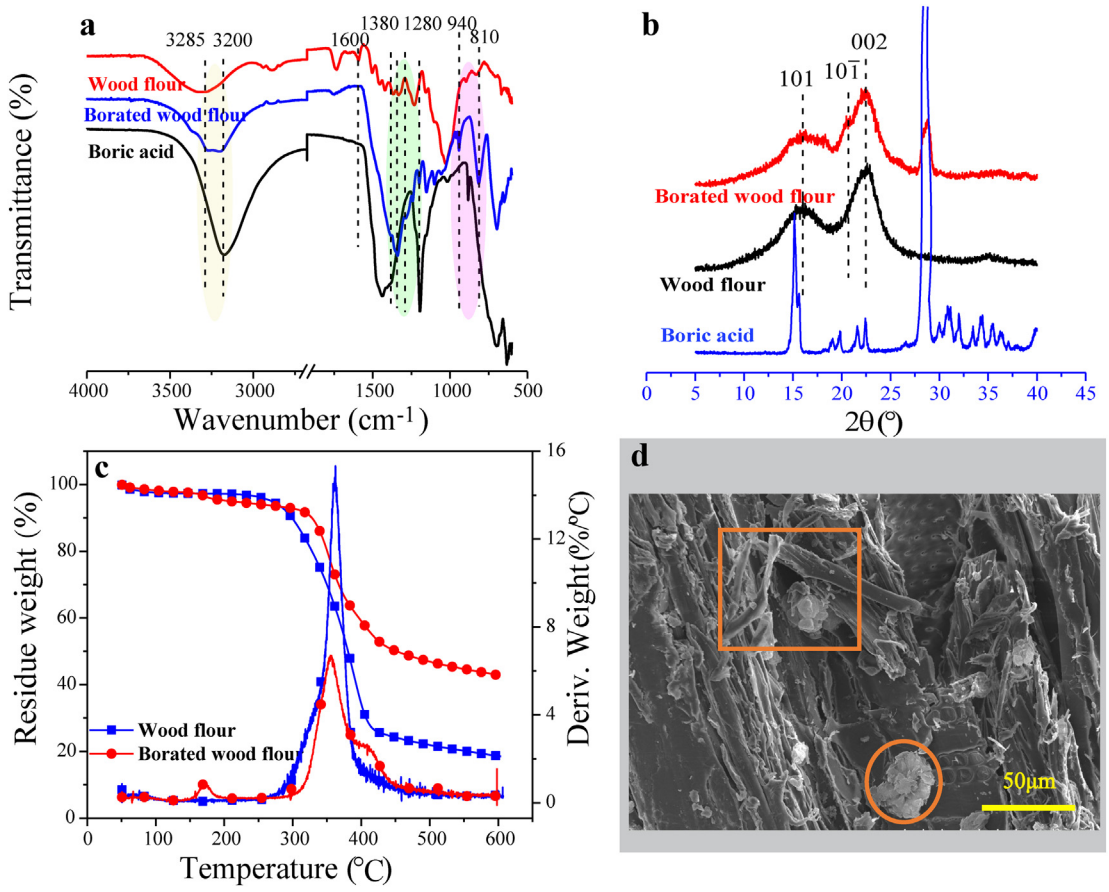


**Fig. 1.** a) FTIR spectra of wood flour, borated wood flour, and boric acid; b) XRD spectra of wood flour, borated wood flour and boric acid; c) TGA and DTG curves of wood flour and borated wood flour; d) Micro-morphology of borated wood flour.

evenly distributed in the borated wood cell walls (Fig. 2), whereas there was no boron in the pure wood flour (Fig. S2). Furthermore, the distribution of the boron elements was very consistent with the position of the carbon and oxygen elements. However, the boron elements aggravated at the position where glassy boron films remained on the surface.

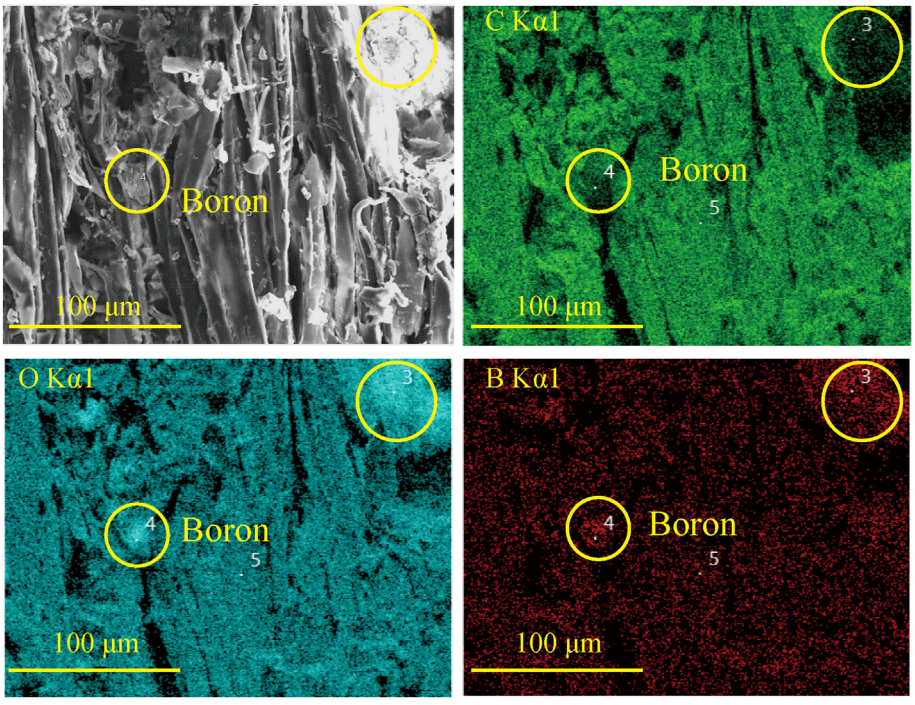


**Fig. 2.** SEM-EDS elemental mapping of borated wood flour.

### 3.2. Properties of the wood flour/PA 6 composites

#### 3.2.1. Micro-morphology of the resulting composites

The fracture surface of pure PA 6 was smooth while wood flour was found in the composites (Fig. 3a and e). The amount of wood flour on the fracture surface increased with increasing wood flour content in the composites (Fig. 3b, c, and d). Wood flour was randomly oriented and formed interconnecting network structure when its content was 50% (Fig. 3d), which is conducive to the modulus of elasticity for composites. However, some voids were observed in WPA50 due to the thermal degradation of the wood flour (Fig. S3a), which has a negative influence on the composites' properties. Furthermore, the wood flour was well wetted by the PA 6 resin and there was no obvious boundary between wood flour and polymer (Fig. 3f, g, and h). This indicates that the interfacial adhesion between the wood flour and PA 6 was very good. It can be explained by the fact that they have similar chemical polarity property and the hydrogen bonds of amide groups and hydroxyl groups formed between the PA 6 chains and the wood flour. Besides, most of the wood flour on the fracture surface was pulled off when the composites were damaged. Fig. 3h shows that boric acid does not influence the interface compatibility between borated wood flour and PA 6. However, some glassy boron oxide films were found in the resin matrix (Figs. 3h & S3b). These boron oxide films were peeled off from the borated wood flour surface due to the shear force. However, it was virtually impossible to observe the size of wood flour in the resulting composites from the SEM photographs because of their complex structure.

The wood flour in the resulting composites was extracted via dissolving the PA 6 matrix resin (Fig. S3). There was barely a difference between the wood flour and borated wood flour morphology before combined with PA 6 resin. The wood flour shortened after extrusion and injection for both borated wood flour/PA 6 composites (BWPAC) and wood flour/PA 6 composites (WPAC) because of screw shear stress (Table S2 and Fig. S3) [27]. Furthermore, the higher the wood flour content, the smaller size of the wood flour in composites and the darker color for the composites. This may be due to the increasing friction in the wood flour with increasing volume fraction, leading to high friction heat, then severe wood flour degradation. The color of wood flour for BWPACs was lighter than that for WPACs. This can be explained by the fact that boric acid improved the thermal stability of the wood flour while the length of wood flour in BWPACs was smaller than that in WPACs. Wood flour swelling caused by the infiltration of boric acid solution leads to its low crystallinity and then to a decrease in strength [28]. The alteration of the cellulose crystal form also reduces the strength of the wood flour as shown in the above XRD analysis (Fig. 1b).

#### 3.2.2. Surface color

Surface color of the resulting composites was influenced by both wood flour content and boric acid treatment (Figs. 4 and S5). The lightness of composites decreased with increasing wood flour content for all test samples. The maximum decrease of lightness ($L$) was observed for WPA50 where the lightness decreased by 51.6% as compared to pure PA 6. For WPACs, the lightness decreased rapidly when the wood content was less than 10%. The change in lightness was moderate and almost linear when wood flour content ranged from 20% to 40%. For BWPACs, the lightness decreased when the wood content was less than 30% and it barely altered when wood content increased above 30%. This decrease can be ascribed to the thermal degradation of the wood flour, forming biochar and oxidation products such as quinones. The lightness of BWPACs was greater than that of WPACs, indicating that boric acid slowed down the lightness decrease of the composites. This observation can be explained by the fact that boric acid improves the wood flour thermal stability.

The greatest color difference between WPACs and BWPACs was observed in yellowness ($b^*$). Compared to pure PA 6, the $b^*$ values of BWPACs increased, whereas they decreased for WPACs. The increase can be attributed to the addition of wood flour. Lignin derivatives play an important role in the yellowness of wood flour [29]. However, the degradation of lignin in the wood flour produced quinone derivatives, leading to a dark color and a decrease in yellowness. Boric acid complexed with lignin in wood flour, thereby preventing the thermal degradation of the lignin. A similar phenomenon with boric acid protecting catechol from oxidation (color darkening) was also observed (Fig. S5). Thus, the $b^*$ values of BWPACs were higher than that of both pure PA 6 and WPACs. The redness of composites increased after adding wood flour, which resulted from the chromophoric groups in wood chemistry, especially extractives [29]. The difference in the $a^*$ value of BWPACs and WPACs was not as obvious as for $b^*$. The low extractive content of poplar explains in the above observation. The $\Delta E$ values of the BWPACs were lower than those of the WPACs, indicating that boric acid slowed down the color change of composites caused by the degradation of wood flour.

#### 3.2.3. Thermal properties

Two melting peaks were observed in the DSC curves of the tested samples, indicating the existence of two main crystalline structures (alpha and gamma) for PA 6 (Fig. 5). The sharp peak in the melting curves can be attributed to an alpha crystalline form while the shoulder peak in the lower temperature is ascribed to polyamide gamma crystals for whose thermal stability is lower than that of alpha crystals [11]. It is well known that crystallinity represents the percentage of the crystalline region while melting point is an indication of the size (thickness)

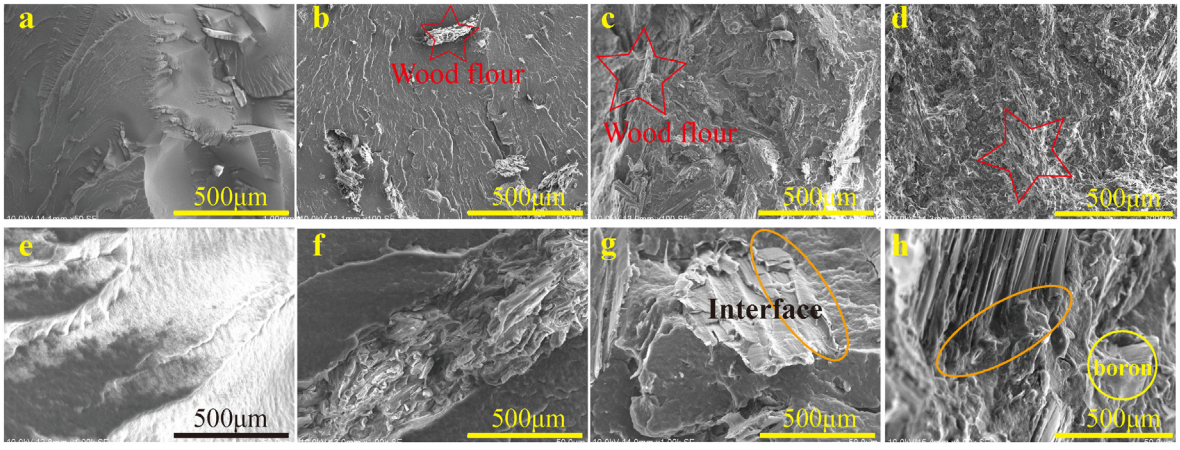


**Fig. 3.** Fracture surface micro-morphology of Pure PA 6 (a & e), wood flour/PA 6 composites containing 10 wt% wood flours (b & f), wood flour/PA 6 composites containing 50 wt% wood flours (e & g), and wood flour/PA 6 composites containing 50 wt% borated wood flours (d & h).

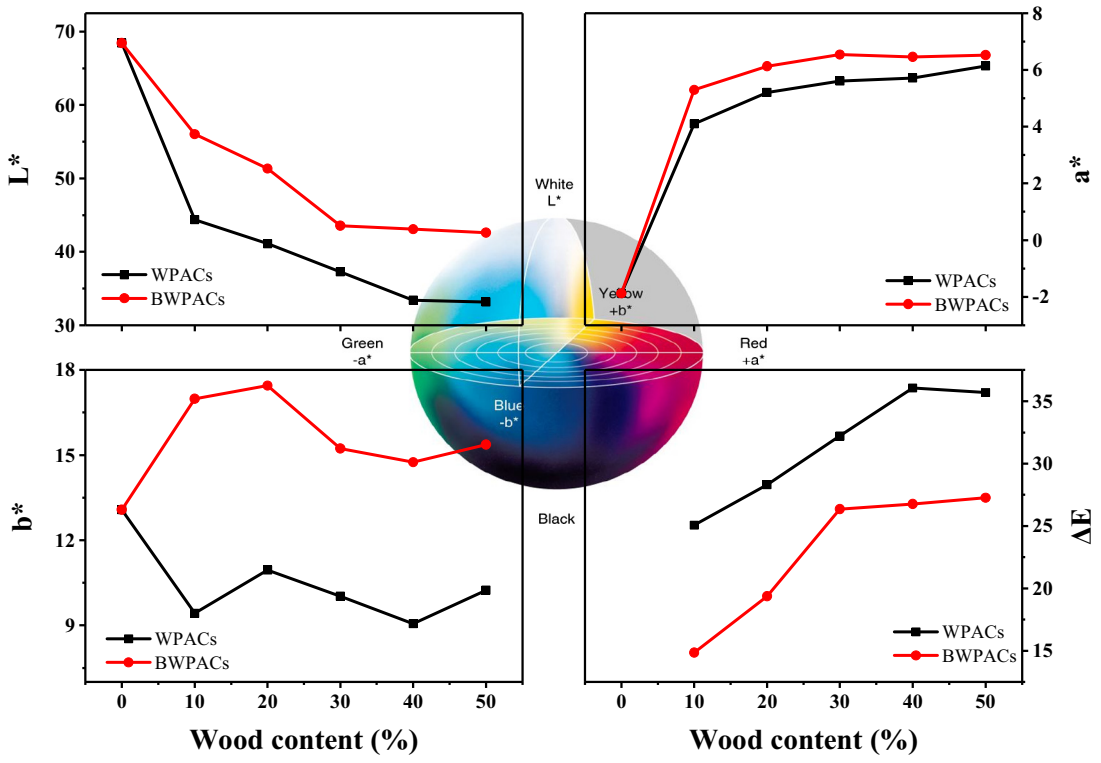


**Fig. 4.** Color changes of treated and untreated-wood flour/PA 6 composites, varying with wood flour content.

of the crystalline region [30]. Both thickness and crystallinity ($X_c$) of the crystals of the tested composites increased first then decreased with increasing wood flour content. This increase is attributed to the nucleating effect of wood flour, which accelerates crystallization. This was also confirmed by the increase in crystallization temperature (Table S3). Similar crystallization behaviors in bio-composites have been extensively

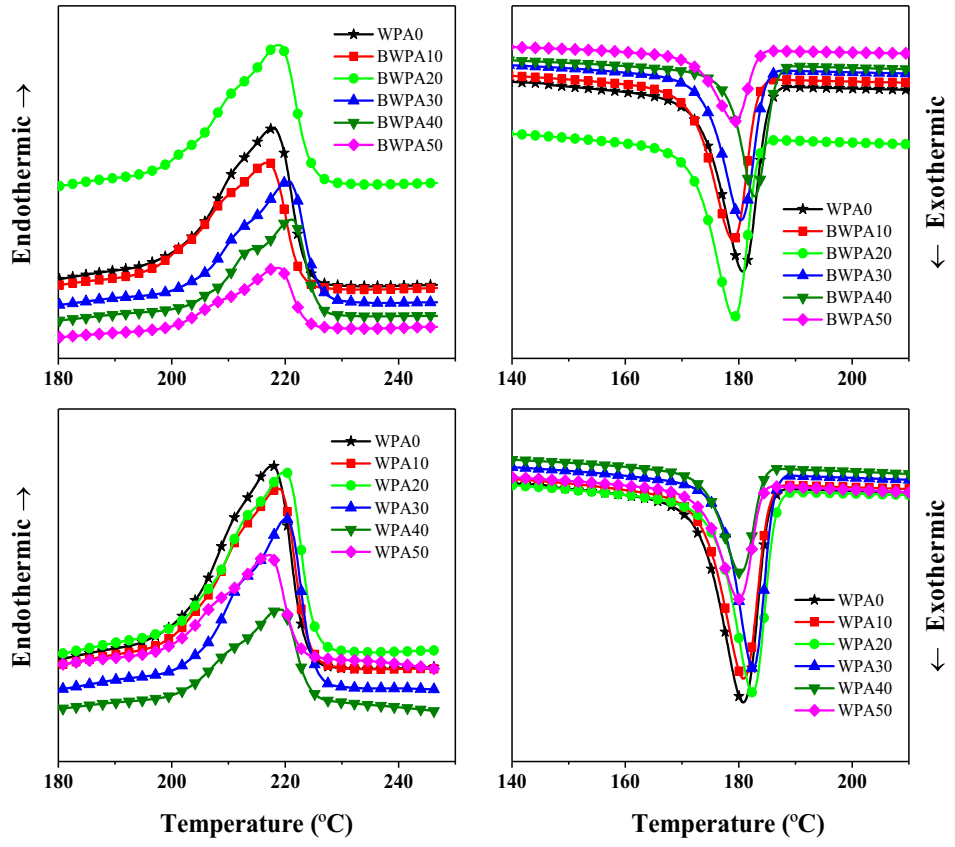


**Fig. 5.** DSC curves of the wood flour/PA 6 composites and the borated wood flour/PA6 composites: the effect of wood flour content.

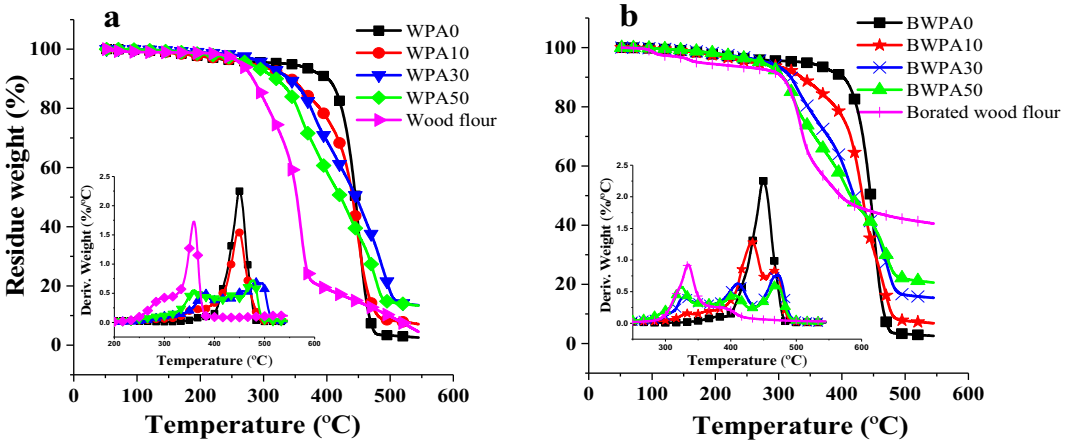


**Fig. 6.** TGA and DTG curves of wood flour/PA 6 composites (a) and borated wood flour/PA 6 composites (b).

reported [4,31]. However, the crystallinity of WPACs deceased after wood flour content was higher than 30%. Wood flour restricted the movement of PA 6 molecular chains, resulting in incomplete crystals. Wood flour can provide nucleating sites for the crystallization of PA 6 but it may also act as a barrier to crystal growth [32].

Furthermore, the results showed that boric acid had a marginally negative effect on composites crystallization. An interfacial interaction between fiber and matrix, as well as their interface shear stress, is believed to be the most influential parameter in transcrystallization [11]. In the current study, boric acid and its self-polymer acted as lubricants, thereby reducing shear stress during processing. Therefore, the crystallization induced by the shear force on the surface of the wood flour was lower for BWPACs than for WPACs. However, the melting temperature and $X_c$ of BWPACs were higher than those of WPACs when the wood content was more than 40%. Wood flour thermal decomposition produces organic volatiles, which have a negative effect on the wood flour and PA 6 matrix interface. However, boric acid slowed down the thermal degradation of wood flour.

Thermogravimetric analysis (TGA) showed that the thermal stability of wood flour was lower than that of the composites (Fig. 6a). The situation was reversed for pure PA 6. The thermal degradation of the composites was due to wood and PA 6 degradation. The temperature at the maximum weight loss rate ($T_{max}$) of the wood flour in the composites was higher than that of pure wood flour due to the fact that the easily degradable components of wood flour, such as hemicellulose and extractives, degraded during processing. The $T_{max}$ of PA 6 increased after being combined to wood flour, whereas its maximum degradation rate decreased. The $T_{max}$ and char residue of WPACs increased with increasing wood flour content. Thus, the higher the wood flour content, the better is the thermal stability of the resulting composites.

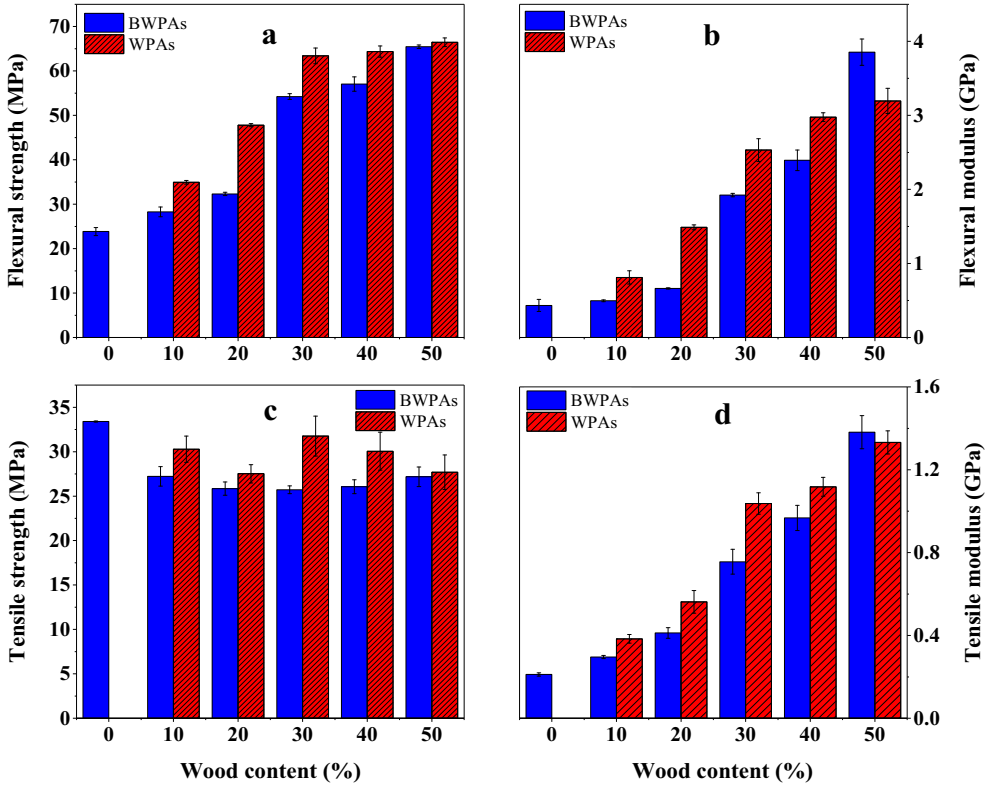


**Fig. 7.** Mechanical properties of the wood flour/PA 6 composites and borated wood flour/PA 6 composites. a) Flexural strength; b) flexural modulus; c) tensile strength; d) tensile modulus.

Furthermore, the actual char residue rate is bigger than that in theory for both WPACs and BWPACs, which revealed that positive interactions between PA and wood flour in thermal stability were present (Fig. S6). The difference between actual and theoretical char residue rates was more obvious for WPACs than for BWPACs. This indicates that the char increase is mostly contributed by wood flour. Wood flour is wrapped by PA 6 polymers, suppressing the escape of volatiles produced from wood degradation then leading to more char formation. On the other hand, the residual carbonaceous layer produced from wood flour thermal degradation provides a thermal isolation layer, slowing down the degradation of the PA 6 [33]. The above results show that wood flour content plays an important role in the thermal stability of the PA 6 based bio-composites. A similar degradation behavior was observed for wood fiber/polypropylene composites [34].

Boric acid not only affected the thermal degradation behavior of the wood flour but also that of the PA 6 (Fig. 6b). The $T_{max}$ of the wood flour in BWPACs decreased compared to the borated wood flour. The decrease can be attributed to the damage of the borated wood flour cross-linked structure during the thermal process. In addition, the degradation of the PA 6 was divided into two stages due to the presence of boric acid (Fig. S7). Boric acid promotes the degradation of PA 6, resulting in a low degradation temperature. However, boric acid may have formed complexation with the amino groups of PA 6. The second degradation peak of PA 6 may contribute to the degradation of the boron-amino complexation. At a certain wood flour content, the char residue of BWPACs was bigger than that of WPACs, indicating boric acid increased the char residue rate of the resulting composites.

### 3.2.4. Mechanical properties

Composite flexural strength and modulus of elasticity increased with the increase of wood flour content, regardless of whether the wood flour was treated or not by boric acid (Fig. 7). An increase of 174.5% was attained for flexural strength, from 23.8 MPa for WPA0 to 65.4 MPa for WPA50 (Fig. 7a). This increase is ascribed to the bridging effect of wood flour [35]. The stress was transmitted between the wood flour and PA 6 resin through the interfacial shear force. An increase of 294% for the flexural modulus of elasticity was observed in BWPA50 (Fig. 7b). This modulus increase is ascribed to the stiffness of the wood flour. Also, wood flour restricted the movement and deformation of the PA 6 matrix resin due to hydrogen bonding and physical crosslinking as shown in Fig. S8, which also contributed to the increase in the modulus. The flexural strength and modulus of BWPACs were lower than those of WPACs, especially in the case of low wood flour content, indicating that boric acid has a negative influence on mechanical properties. This can be explained by the fact that boric acid treatments change the crystalline behavior of wood flour and reduce its strength. On the other hand, the size of the wood flour in BWPACs was smaller than that in WPACs. Wood flour size is known to be one of the most

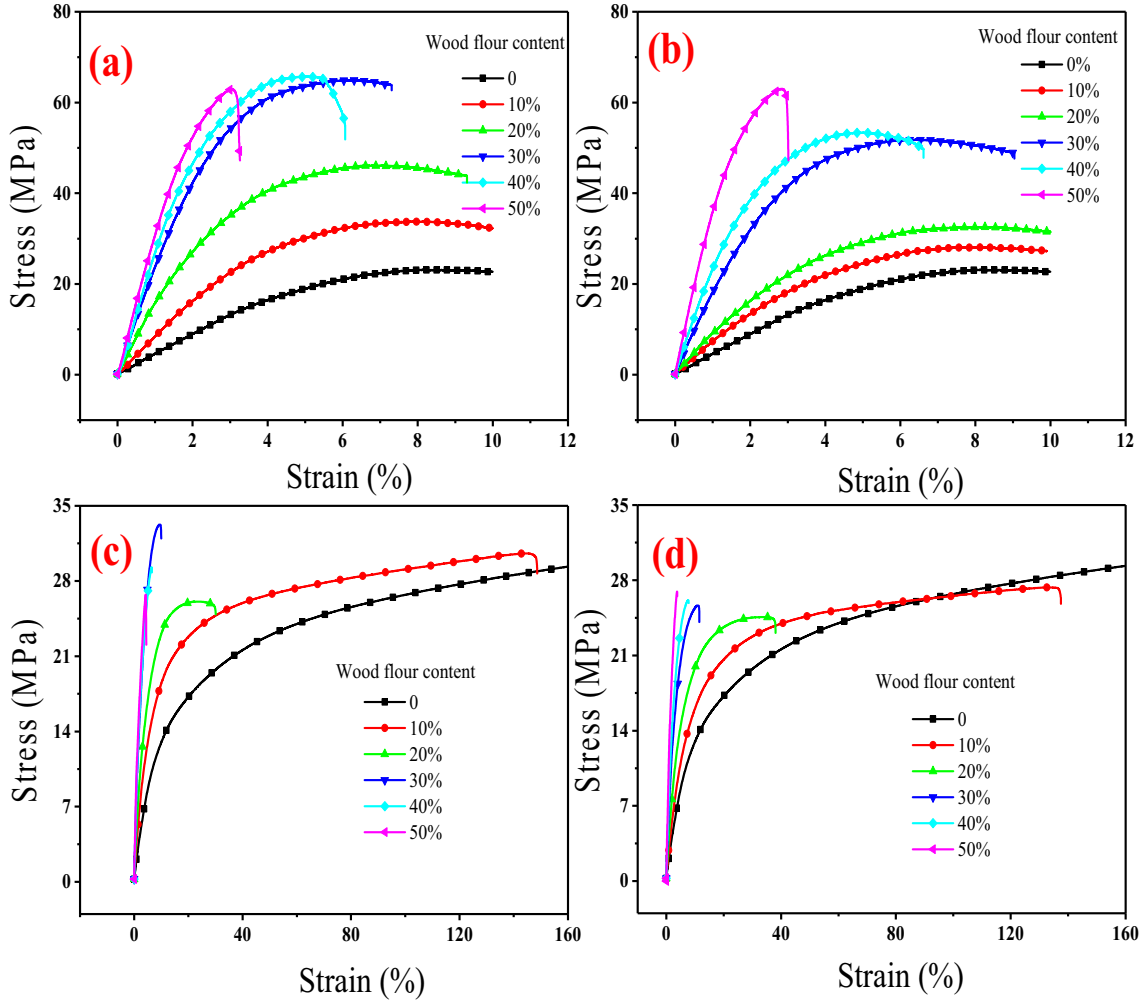


**Fig. 8.** Stress-strain curves of wood flour/PA 6 composites (a) and borated wood flour/PA 6 composites (b) in three-point flexural tests, and stress-nominal strain curves of wood flour/PA 6 composites (c) and borated wood flour/PA 6 composites (d) in tensile tests.

influential parameters for the mechanical properties of bio-composites [36].

It is worth noting that the difference in flexural properties between BWPACs and WPACs decreased with an increase of wood flour content. The flexural modulus of BWPA50 was even higher than that of WPA50. High wood flour content would promote friction heat, resulting in further degradation of wood flour followed by decreases in wood flour strength. Besides, wood thermal degradation generated volatile organic compounds, leading to a decrease in composites strength. However, the boric acid treatment improved the thermal stability of wood flour, preventing the decrease in wood flour strength caused by thermal degradation.

Fig. 7c and d show the effects of wood content and boric acid on the tensile performance of the resulting composites. The variation in the tensile modulus of elasticity of the composites with wood content was similar to that of the flexural modulus of elasticity (Fig. 7d). The increase of the tensile modulus of elasticity was also due to the limitation of wood flour on the movement and deformation of the PA 6 chains. In this case, the crack propagation mechanism was dominant instead of the dissipation energy mechanism of plastic deformation under external energy. This could also explain the decrease of elongation rate with an increase in wood flour content (Fig. S9). Furthermore, break strain of the resulting composites decreased with increasing wood flour content in both flexural and tensile tests (Fig. 8). However, the tensile strength of the resulting composites showed decreasing trends with increasing wood flour content (Fig. 7c). Tensile strength is not only influenced by the intensity of interfacial adhesion but is also affected by the softness of the interface between the resin matrix and the filler [37]. The reduction in tensile strength may primarily due to the weak interface resulted from the agglomeration of wood flour which initiates failure under stress. Moreover, the wood flour restricted the mobility of PA 6 chains and destroyed the original toughening effect for the toughened nylon-6.

## 4. Conclusions

Boric acid can react with wood flour through complexation or esterification, which promotes thermal stability in wood flour. Boric acid slowed down the discoloration of bio-composites and was beneficial for composite processing. However, boric acid decreased composites strength. A good interfacial adhesion between lignocellulose and polyamide 6 was obtained because of their similar polarity. This study laid the groundwork for future research on preparing lignocellulose-engineered plastic composites through improving the thermal stability of lignocellulose. The knowledge gained from this work and future studies will expand possible uses of biomass materials.

## CRediT authorship contribution statement

**Jingfa Zhang:** Methodology, Investigation, Writing - original draft. **Ahmed Koubaa:** Writing - review & editing, Supervision, Funding acquisition. **Dan Xing:** Investigation. **Wanyu Liu:** Investigation. **Qingwen Wang:** Supervision, Funding acquisition. **XiangMing Wang:** Writing - review & editing. **Haigang Wang:** Methodology, Writing - review & editing.

## Declaration of competing interest

The authors declare that they have no known competing financial interests or personal relationships that could have appeared to influence the work reported in this paper.

## Acknowledgements

This work was financially supported by the Canada Research Chairs, Natural Sciences and Engineering Research Council of Canada and the Fundamental Research Funds for the Central Universities (No. 2572018BB07). The first author Jingfa Zhang (201706600026) is supported by the China Scholarship Council.

## Appendix A. Supplementary data

Supplementary data to this article can be found online at https://doi.org/10.1016/j.matdes.2020.108589.

## References

[1] A. Ashori, Wood–plastic composites as promising green-composites for automotive industries! Bioresour. Technol. 99 (11) (2008) 4661–4667.
[2] B. Mu, H. Wang, X. Hao, Q. Wang, Morphology, mechanical properties and dimensional stability of biomass particles/high density polyethylene composites: effect of species and composition, Polymers 10 (3) (2018) 308.
[3] S. Xu, Y. Fang, S. Yi, J. He, X. Zhai, Y. Song, H. Wang, Q. Wang, Effects of lithium chloride and chain extender on the properties of wood fiber reinforced polyamide 6 composites, Polym. Test. 72 (2018) 132–139.
[4] A. Kiziltas, B. Nazari, D.J. Gardner, D.W. Bousfield, Polyamide 6–cellulose composites: effect of cellulose composition on melt rheology and crystallization behavior, Polym. Eng. Sci. 54 (4) (2014) 739–746.
[5] S. Xu, Y. Fang, S. Yi, J. He, X. Zhai, H. Wang, Q. Wang, Impact of lithium chloride and in-situ grafting on the performance of microcrystalline cellulose-filled composites based on polyamide 6/high-density polyethylene, Polym. Compos. 40 (S1) (2019) E865–E876.
[6] C. Klason, J. Kubat, H.-E. Strömvall, The efficiency of cellulosic fillers in common thermoplastics. Part 1. Filling without processing aids or coupling agents, Int. J. Polym. Mater. 10 (3) (1984) 159–187.
[7] H. Yousefian, D. Rodrigue, Effect of nanocrystalline cellulose on morphological, thermal, and mechanical properties of nylon 6 composites, Polym. Compos. 37 (5) (2016) 1473–1479.
[8] A. Buchenauer, Wood Fiber Polyamide Composites for Automotive Applications, University of Waterloo, 2016.
[9] D. Aydemir, A. Kiziltas, E.E. Kiziltas, D.J. Gardner, G. Gunduz, Heat treated wood–nylon 6 composites, Compos. Part B 68 (2015) 414–423.
[10] P.A. Santos, M.A. Spinacé, K.K. Fermoselli, M.-A. De Paoli, Polyamide-6/vegetal fiber composite prepared by extrusion and injection molding, Compos. A: Appl. Sci. Manuf. 38 (12) (2007) 2404–2411.
[11] Y. Amintowlieh, A. Sardashti, L.C. Simon, Polyamide 6–wheat straw composites: effects of additives on physical and mechanical properties of the composite, Polym. Compos. 33 (6) (2012) 976–984.
[12] R. Pedieu, A. Koubaa, B. Riedl, X.-M. Wang, J. Deng, Fire-retardant properties of wood particleboards treated with boric acid, Eur. J. Wood Wood Prod. 70 (1–3) (2012) 191–197.
[13] A. Donmez Cavdar, F. Mengeloğlu, K. Karakus, Effect of boric acid and borax on mechanical, fire and thermal properties of wood flour filled high density polyethylene composites, Measurement 60 (2015) 6–12.
[14] Q. Wang, J. Li, J. Winandy, Chemical mechanism of fire retardance of boric acid on wood, Wood Sci. Technol. 38 (5) (2004).
[15] B. Wicklein, D. Kocjan, F. Carosio, G. Camino, L. Bergström, Tuning the nanocellulose–borate interaction to achieve highly flame retardant hybrid materials, Chem. Mater. 28 (7) (2016) 1985–1989.
[16] I.H. Uner, I. Deveci, E. Baysal, T. Turkoglu, H. Toker, H. Peker, Thermal analysis of Oriental beech wood treated with some borates as fire retardants, Maderas, Ciencia y Tecnología 18 (2) (2016) 293–304.
[17] M. Usman, H. Chen, K. Chen, S. Ren, J.H. Clark, J. Fan, G. Luo, S. Zhang, Characterization and utilization of aqueous products from hydrothermal conversion of biomass for bio-oil and hydro-char production: a review, Green Chem. 21 (7) (2019) 1553–1572.
[18] C. Chio, M. Sain, W. Qin, Lignin utilization: a review of lignin depolymerization from various aspects, Renew. Sust. Energ. Rev. 107 (2019) 232–249.
[19] L. Segal, J. Creely, A. Martin Jr., C. Conrad, An empirical method for estimating the degree of crystallinity of native cellulose using the X-ray diffractometer, Text. Res. J. 29 (10) (1959) 786–794.
[20] N. Feng, A. Zheng, Q. Wang, P. Ren, X. Gao, S.-B. Liu, Z. Shen, T. Chen, F. Deng, Boron environments in B-doped and (B, N)-codoped TiO2 photocatalysts: a combined solid-state NMR and theoretical calculation study, J. Phys. Chem. C 115 (6) (2011) 2709–2719.
[21] S. Xia, S. Gao, J. LI, W. Li, IR-spectra of borate, J. Salt Lake Sci. 3 (3) (1995) 49–53.
[22] E.N. Boulos, N. Kreidl, Structure and properties of silver borate glasses, J. Am. Ceram. Soc. 54 (8) (1971) 368–375.
[23] K.M.A. Uddin, M. Ago, O.J. Rojas, Hybrid films of chitosan, cellulose nanofibrils and boric acid: flame retardancy, optical and thermo-mechanical properties, Carbohydr. Polym. 177 (2017) 13–21.
[24] A. El Oudiani, Y. Chaabouni, S. Msahli, F. Sakli, Crystal transition from cellulose I to cellulose II in NaOH treated Agave americana L. fibre, Carbohydr. Polym. 86 (3) (2011) 1221–1229.
[25] F.J. Kolpak, J. Blackwell, Determination of the structure of cellulose II, Macromolecules 9 (2) (1976) 273–278.
[26] Z. Xiao, S. Liu, Z. Zhang, C. Mai, Y. Xie, Q. Wang, Fire retardancy of an aqueous, intumescent, and translucent wood varnish based on guanylurea phosphate and melamine-urea-formaldehyde resin, Prog. Org. Coat. 121 (2018) 64–72.

[27] N. Graupner, K. Albrecht, G. Ziegmann, H. Enzler, J. Müssig, Influence of reprocessing on fibre length distribution, tensile strength and impact strength of injection moulded cellulose fibre-reinforced polylactide (PLA) composites, Express Polym Lett 10 (8) (2016) 647.
[28] G. Colakoglu, S. Colak, I. Aydin, U.C. Yildiz, S. Yildiz, Effect of boric acid treatment on mechanical properties of laminated beech veneer lumber, Silva Fenn 37 (4) (2003) 505–510.
[29] L. Persze, L. Tolvaj, Photodegradation of wood at elevated temperature: colour change, J. Photochem. Photobiol. B 108 (2012) 44–47.
[30] A.R. Bhattacharyya, P. Pötschke, L. Häußler, D. Fischer, Reactive compatibilization of melt mixed PA6/SWNT composites: mechanical properties and morphology, Macromol. Chem. Phys. 206 (20) (2005) 2084–2095.
[31] S. Rohner, J. Humphry, C.M. Chaléat, L.-J. Vandi, D.J. Martin, N. Amiralian, M.T. Heitzmann, Mechanical properties of polyamide 11 reinforced with cellulose nanofibres from Triodia pungens, Cellulose 25 (4) (2018) 2367–2380.
[32] F. Xin, L. Li, The role of a silane coupling agent in carbon nanotube/polypropylene composites, J. Compos. Mater. 46 (26) (2012) 3267–3275.
[33] A.A. Klyosov, Wood-Plastic Composites, John Wiley &Sons Inc, 2007.
[34] J.G. Gwon, S.Y. Lee, J.H. Kim, Thermal degradation behavior of polypropylene base wood plastic composites hybridized with metal (aluminum, magnesium) hydroxides, J. Appl. Polym. Sci. 131 (7) (2014)(n/a-n/a).
[35] P. Amuthakkannan, V. Manikandan, J.W. Jappes, M. Uthayakumar, Effect of fibre length and fibre content on mechanical properties of short basalt fibre reinforced polymer matrix composites, Mater. Phys. Mech. 16 (2) (2013) 107–117.
[36] H. Bouafif, A. Koubaa, P. Perré, A. Cloutier, Effects of fiber characteristics on the physical and mechanical properties of wood plastic composites, Compos. A: Appl. Sci. Manuf. 40 (12) (2009) 1975–1981.
[37] M. Biswal, S. Mohanty, S.K. Nayak, P.S. Kumar, Effect of functionalized nanosilica on the mechanical, dynamic-mechanical, and morphological performance of polycarbonate/nanosilica nanocomposites, Polym. Eng. Sci. 53 (6) (2013) 1287–1296.